

Electronic Supporting Information
for

Kinetic Effects of Tartaric Acid on the Growth of Chiral J-Aggregates of tetrakis(4-sulfonatophenyl)porphyrin

Maria Angela Castriciano,^{* a} Andrea Romeo,^{a,b} Roberto Zagami,^b Norberto Micali^c and Luigi Monsù Scolaro^{* a,b}

^aCNR-ISMN, Istituto per lo Studio dei Materiali Nanostrutturati, 98166, V.le F. Stagno D'Alcontres 31 Messina, Italy. ^bDipartimento di Chimica Inorganica, Chimica Analitica e Chimica Fisica, and C.I.R.C.M.S.B., University of Messina, V.le F. Stagno D'Alcontres 31, Vill. S. Agata, 98166 Messina, Italy.
^cCNR-IPCF, Istituto per i Processi Chimico-Fisici, 98158, V.le F. Stagno d'Alcontres 37 Messina, Italy.

Experimental section

5,10,15,20-tetrakis(4-sulfonatophenyl)porphyrin (H_2TPPS_4) tetra-sodium salt was purchased from Aldrich Co. Aqueous stock solutions of this porphyrin (300 μM) were prepared in dust-free Millipore water, stored in the dark and freshly used. Porphyrin concentration has been determined spectrophotometrically by using $\epsilon_{414} = 5.33 \times 10^5 \text{ M}^{-1}\text{cm}^{-1}$ at the Soret maximum in water. High purity D (99%), L (99.5%) and meso (98%) tartaric acid, R (98%) and S (99%) camphorsulfonic acid, and hydrochloridric acid were purchased from Aldrich Co. D and L tartaric acid were recrystallized several times from hot water (purity has been checked through circular dichroism and ^1H NMR spectroscopy, see Fig. S1); R and S camphorsulfonic acid were recrystallized several times from glacial acetic acid. Being the aggregate structures strongly affected by the mixing order of reagents, aggregated porphyrin samples were prepared by addition of the proper amount of concentrated chiral acid to a diluted porphyrin solution, followed by the rapid addition of HCl.

Methods. UV/Vis spectra were collected using a Hewlett-Packard mod. 8453 diode array spectrophotometer using 0.1 - 1 cm pathlength quartz cells. Kinetic experiments were carried out in the thermostated compartment of the spectrophotometer, with a temperature accuracy of ± 0.1 K.

The analysis of the kinetic profiles has been performed by a non-linear fit of the absorption data according equation 1 (ref. 16 in the text):

$$\text{Ext} = \text{Ext}_{\infty} + (\text{Ext}_0 - \text{Ext}_{\infty}) (1 + (m - 1)\{k_0 t + (n + 1)^{-1} (k_c t)^{n+1}\})^{-1/(m-1)} \quad \text{equation 1}$$

with Ext_0 , Ext_{∞} , k_0 , k_c , m and n as the parameters to be optimized (Ext , Ext_0 and Ext_{∞} are the extinction at time t , at starting time and at the end of aggregation, respectively).

The circular dichroism (CD) spectra were recorded on a JASCO J-720 spectropolarimeter, equipped with a 450 W xenon lamp. The ellipticity was obtained by calibrating the instrument with a 0.06% aqueous solution of R-camphorsulfonic acid. CD spectra were corrected both for the cell and solvent contributions.

^1H NMR spectra were obtained on a Bruker Avance 300 spectrometer equipped with a broadband probe operating at 300.13 MHz. Sample solutions in $\text{dmso}-d_6$ were referenced to the internal residual solvent peak. Chemical shifts (δ) are reported in p.p.m. downfield from TMS.

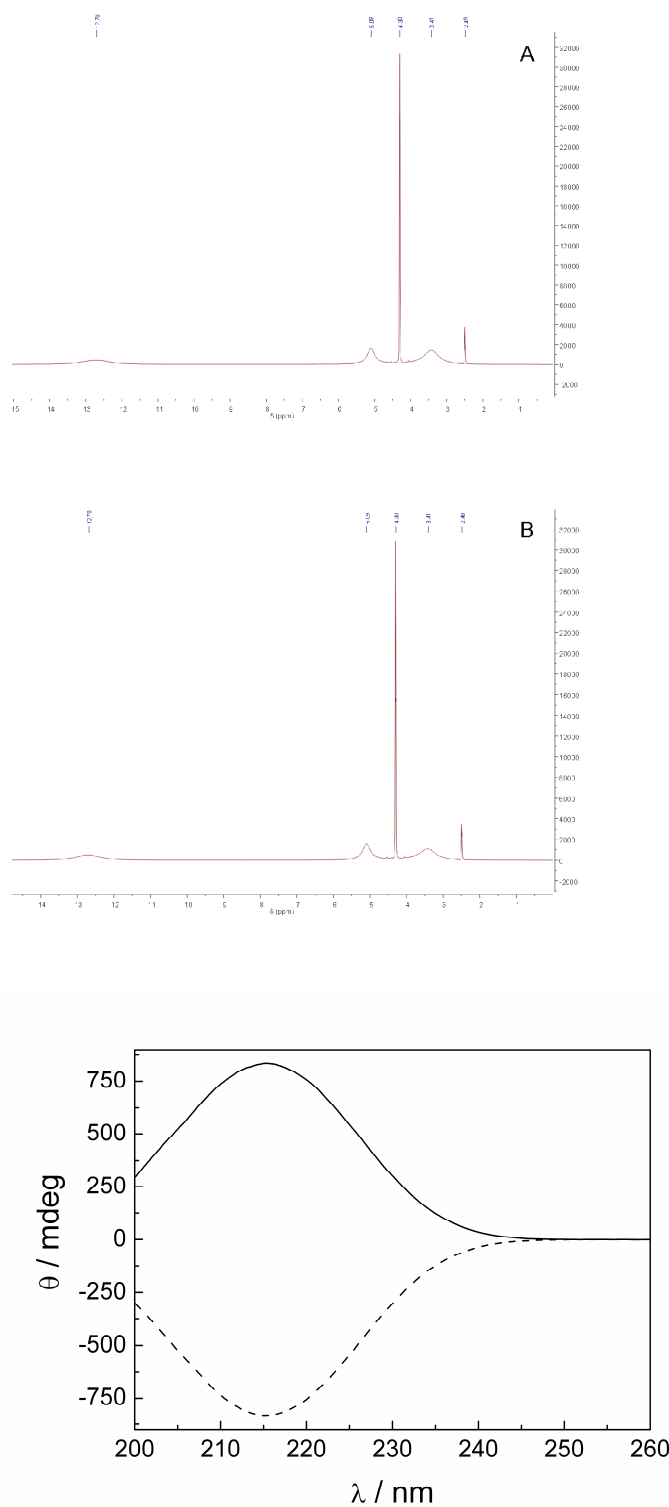


Figure S1. ¹H NMR spectra (upper plots) of D (A) and L (B) tartaric acid 0.2 M in dmso-*d*₆. CD spectra (lower plot) of D (solid line) and L (dashed line) tartaric acid. [tartaric acid] = 5 mM; $\Delta\epsilon/\epsilon = 2 \times 10^{-2}$ (834 mdeg at 216 nm) and $\Delta\epsilon/\epsilon = -2 \times 10^{-2}$ (-832 mdeg at 216 nm) for D and L tartaric acid, respectively.

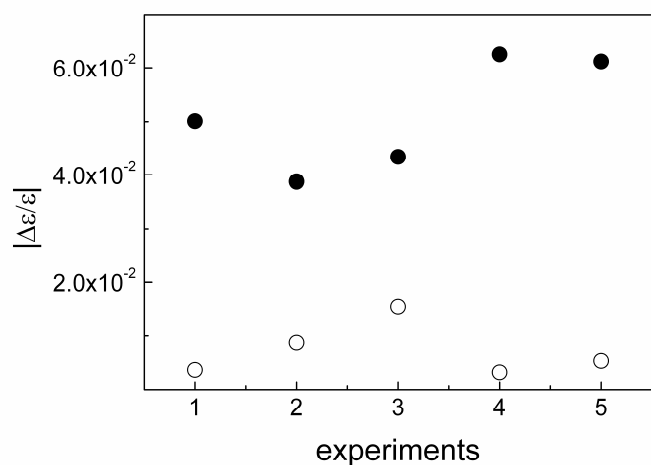


Figure S2. $|\Delta\varepsilon/\varepsilon|$ for H_4TPPS_4 J-aggregates induced by HCl in presence of D or L-tartaric acid.

$[\text{H}_4\text{TPPS}_4] = 3 \mu\text{M}$; [tartaric acid] = 100 mM; [HCl] = 0.5 M; T = 298 K.

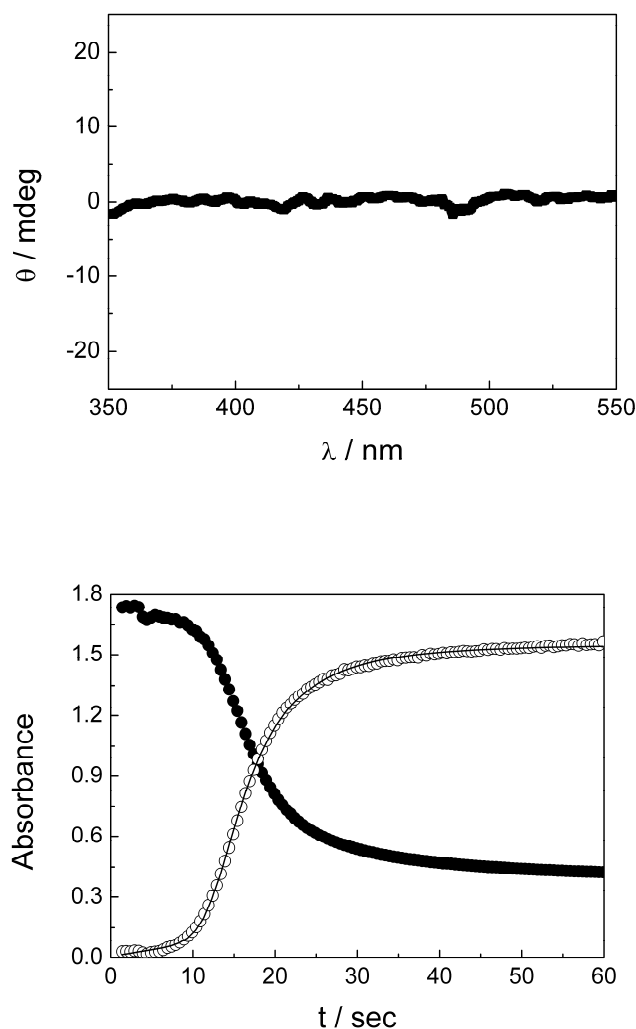


Figure S3. CD spectrum (upper) and the corresponding absorption kinetic profile $\lambda = 434 \text{ nm}$ (full circles); $\lambda = 491 \text{ nm}$ (empty circles) (lower) for H_4TPPS_4 J-aggregates induced by HCl in the presence of *meso*-tartaric acid. $[\text{H}_4\text{TPPS}_4] = 20 \mu\text{M}$; [*meso*-tartaric acid] = 100 mM; [HCl] = 0.5 M; optical path length 2 mm, $T = 298 \text{ K}$. The solid lines are the best-fits of the experimental data ($\square_{491\text{nm}}$) to Pasternack's autocatalytic model (equation 1): $k_0 = (4.3 \pm 0.08) \times 10^{-3} \text{ s}^{-1}$; $k_c = (8.6 \pm 0.02) \times 10^{-2} \text{ s}^{-1}$; $m = 3.4 \pm 0.1$; $n = 6.8 \pm 0.2$; $R^2 = 0.9997$.

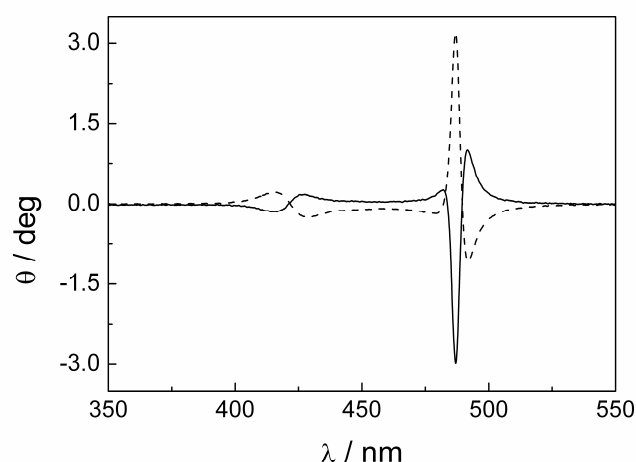


Figure S4. CD spectra for H_4TPPS_4 J-aggregates induced by addition of H_2SO_4 in the presence of D (solid line) or L (dashed line) tartaric acid according to the procedure reported in Y. Kitagawa, H. Segawa and K. Ishii *Angew. Chem. Int. Ed.* 2011, **50**, 9133.

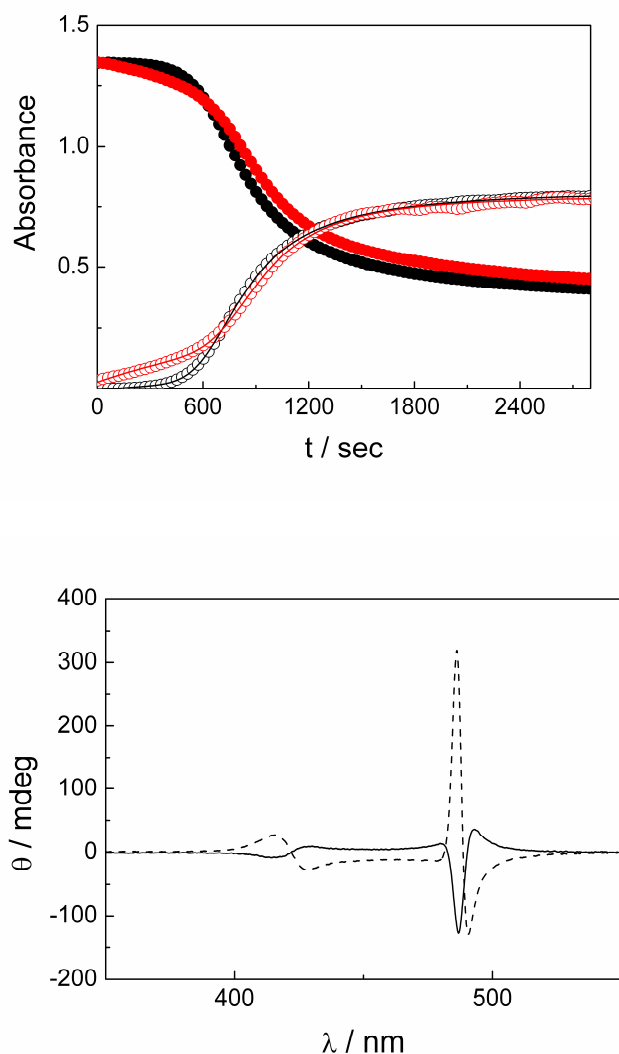


Figure S5. Absorption kinetic profiles (upper) and final CD spectra (lower) for H_4TPPS_4 aggregation induced by H_2SO_4 in presence of L-tartaric acid (red points and dashed lines) and D-tartaric acid (black points and solid lines). $[\text{H}_4\text{TPPS}_4] = 3 \mu\text{M}$; [tartaric acid] = 100 mM; $[\text{H}_2\text{SO}_4] = 0.5 \text{ M}$, $\lambda = 434 \text{ nm}$ (full circles black or red); $\lambda = 491 \text{ nm}$ (empty circles black or red); $T = 298 \text{ K}$. $|\Delta\epsilon/\epsilon| = 1.7 \times 10^{-2}$ and 0.6×10^{-2} for L and D enantiomers, respectively. The solid lines are the best-fits of the experimental data ($\lambda = 491 \text{ nm}$) to Pasternack's autocatalytic model (equation 1): (L-tartaric acid: $k_0 = (3.3 \pm 0.02) \times 10^{-4} \text{ s}^{-1}$; $k_c = (1.5 \pm 0.01) \times 10^{-3} \text{ s}^{-1}$; $m = 3.4 \pm 0.2$; $n = 6.7 \pm 0.4$; $R^2 = 0.9991$; D-tartaric acid: $k_0 = (6.9 \pm 0.05) \times 10^{-5} \text{ s}^{-1}$; $k_c = (1.7 \pm 0.01) \times 10^{-3} \text{ s}^{-1}$; $m = 3.7 \pm 0.05$; $n = 6.2 \pm 0.1$; $R^2 = 0.9999$).

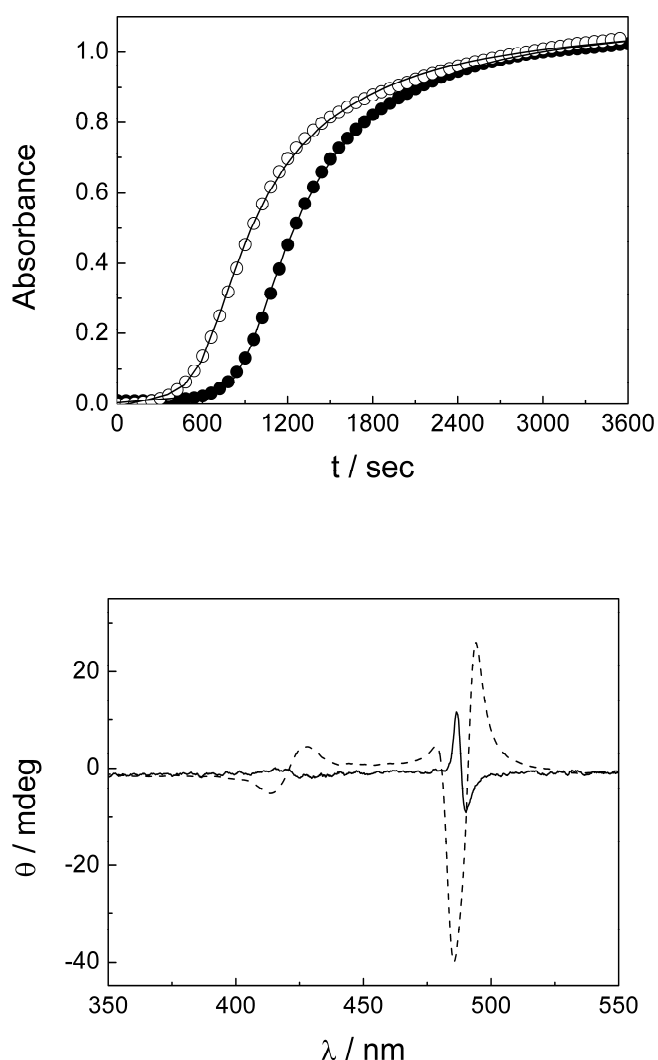


Figure S6. Absorption kinetic profiles (upper) and final CD spectra (lower) for H_4TPPS_4 aggregation induced by *R*-camphorsulfonic acid (empty circle points and dashed line) or *S*-camphorsulfonic acid (full circle points and solid line). $[\text{H}_4\text{TPPS}_4] = 40 \mu\text{M}$; [camphorsulfonic acid] = 50 mM; optical path length 2 mm; $T = 298 \text{ K}$. $|\Delta\epsilon/\epsilon| = 1.9 \times 10^{-3}$ and 6.1×10^{-4} for *R* and *S* enantiomers, respectively. The solid lines are the best-fits of the experimental data ($\lambda_{491\text{nm}}$) to Pasternack's autocatalytic model (equation 1). *S*-camphorsulfonic acid: $k_0 = (3.0 \pm 0.6) \times 10^{-5} \text{ s}^{-1}$; $k_c = (1.1 \pm 0.02) \times 10^{-3} \text{ s}^{-1}$; $m = 5.9 \pm 0.2$; $n = 9.4 \pm 0.3$; $R^2 = 0.9998$. *R*-camphorsulfonic acid: $k_0 = (8.0 \pm 0.6) \times 10^{-5} \text{ s}^{-1}$; $k_c = (1.6 \pm 0.01) \times 10^{-3} \text{ s}^{-1}$; $m = 5.5 \pm 0.4$; $n = 6.1 \pm 0.5$; $R^2 = 0.9997$.

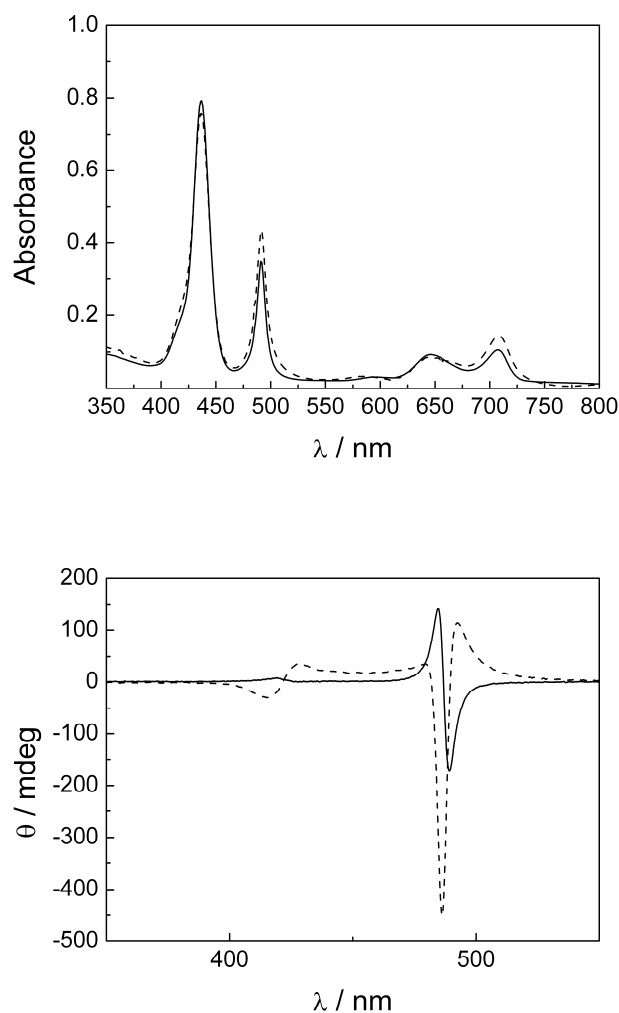


Figure S7. UV/Vis absorption (upper) and CD (lower) spectra for H_4TPPS_4 J-aggregates induced by addition of HCl in presence of *S* (solid line) or *R* (dashed line) camphorsulfonic acid. $[\text{H}_4\text{TPPS}_4] = 3 \mu\text{M}$; [camphorsulfonic acid] = 100 mM; $[\text{HCl}] = 0.5 \text{ M}$; $T = 298 \text{ K}$. $|\Delta\epsilon/\epsilon| = 2.7 \times 10^{-2}$ and 3.9×10^{-2} for *S* and *R* enantiomers, respectively.